Macromolecules

COMMUNICATION TO THE EDITOR

pubs.acs.org/Macromolecules

Unusual Crystallization Behavior of Polyethylene Having Precisely Spaced Branches

Yoshinobu Nozue,*[,†] Yasutoyo Kawashima,[†] Shuichiro Seno,[†] Tatsuhiro Nagamatsu,[†] Satoru Hosoda,[†,&] Erik B. Berda,[‡,§] Giovanni Rojas,[‡,∥] Travis W. Baughman,[‡,⊥] and Kenneth B. Wagener*[,‡]

[†]Petrochemicals Research Laboratory, Sumitomo Chemical Co., Ltd., Kitasode, Chiba, Japan

[‡]Department of Chemistry, University of Florida, Gainesville, Florida 32611-7200, United States

Supporting Information

The importance of a metastable mesophase has been widely reported in many soft condensed-matter systems. In *n*-alkanes, C_nH_{2n+2}, a rotator phase, which is considered as a crystal with molecular disorder, appears. Its structure and stability are strongly dependent on the chain length and the temperature.[1−3] In *n*-alkanes with an even number of carbon atoms, *n*, and $n < 18$, the rotator phase appears transiently as a mesophase prior to formation of a triclinic crystalline domain.[4]

When a polyester crystallizes under cold crystallization conditions, concentration fluctuations have been observed prior to crystallization by small- and wide-angle X-ray scattering measurements.[5,6] In the reports, SAXS peak development was observed prior to the emergence of crystalline Bragg peaks in WAXS. The manner of SAXS growth in the initial stage was explained by the Cahn−Hilliard theory for spinodal decomposition. The concentration fluctuations were apparently the result of a spinodal decomposition process between the isotropic melt and the ordered mesophase domains.

Viewed from a different perspective, a mesophase-mediated crystallization mechanism other than spinodal decomposition-assisted crystallization has been proposed by Keller and co-workers. They suggest that a hexagonal phase appears as a metastable mesophase in PE under certain pressure and temperature conditions and that the crystal thickness increases significantly followed by the subsequent crystal transformation to an orthorhombic phase.[7,8] They discussed this phenomenon using a $T-l^{-1}$ phase diagram (where *l* means the layer thickness of the mesophase or crystals). Initially, a small-sized hexagonal phase, the free energy of which is lower than that of an orthorhombic phase of the same size in the range of small *l*, is formed, and layer thickening and lateral growth follow. During this size-up process, the state of PE in the phase diagram moves from the hexagonal phase-favored region to the orthorhombic phase-favored region. Recently, Strobl and co-workers have suggested a novel crystallization mechanism by using the concept of the $T-l^{-1}$ phase diagram. In their model, a small-sized mesomorphic layer appears near the interface of the crystal growth front in the first stage. The mesomorphic layer gradually grows along the chain axis and sequentially transforms to native and lamellar crystals.[9] In general, however, the role and importance of the ordered mesophase in crystalline polymers are still shrouded in mystery.

This paper reports evidence for a transient ordered mesophase in the crystallization of PE with short chain branches (SCB) placed at precise intervals along the chain. The branched PE samples were synthesized by ADMET polymerization technology[10−13] with either ethyl branches precisely spaced on every 21st carbon (EB21) or with hexyl branches on every 21st carbon (HB21). The weight-averaged molecular weight (M_w) and the distribution (M_w/M_n) were M_w = 33 000 and M_w/M_n = 2.0 in EB21 and M_w = 40 000 and M_w/M_n = 1.55 in HB21. Detailed setups for the following experiments are described in the Supporting Information.

The DSC thermograms of EB21 and HB21 were obtained after heating to 50 °C, cooling to −20 °C at 10 °C/min, and reheating at 10 °C/min, and the thermal profiles show sharp exothermic/endothermic peaks during the cooling/heating segments. The observed transition peak temperatures during cooling (T_c) and heating (T_m) were T_c = 11 °C, ΔH_c = 64.3 J/g, T_m = 24 °C, ΔH_m = 65.0 J/g in EB21 and T_c = 1 °C, ΔH_c = 51.6 J/g, T_m = 12 °C, ΔH_m = 52.0 J/g in HB21. Here, it should be noted that the maximum melting temperatures were about 3−4 °C higher than the peak melting temperature. These results indicate that EB21 and HB21 exhibit first-order phase transitions. Furthermore, polarized optical microscopy (POM) of samples having the same thermal history as those analyzed by DSC showed that a birefringent structure was rapidly formed below the phase transition temperature. Figure 1a,b shows contour plots of SAXS and WAXS profile changes for EB21 obtained at a cooling rate of 10 °C/min. Corresponding WAXS pattern changes are shown in movie 1a. The behavior is very similar to that in HB21 (see movie 1b). The SAXS and WAXS pattern changes gradually start at 18−19 °C. The structure having a long period and denser packing than the amorphous phase is already formed at the phase transition temperature determined by DSC, and the change in packing structure occurs rapidly and cooperatively. Interestingly, the observed WAXS change was only the appearance at larger angle of a broad peak, which is narrower in width than that of the amorphous phase; any sharp Bragg peak indicative of ordered crystal formation was not detected during cooling. The peak position of WAXS (∼1.49−1.53 $Å^{-1}$) originating from this phase coincides well with that of the hexagonal phase in PE (∼1.52 $Å^{-1}$).[14] In SAXS, the signal increased and the long period was gradually formed during cooling.

Received: January 21, 2011
Revised: March 23, 2011
Published: May 13, 2011

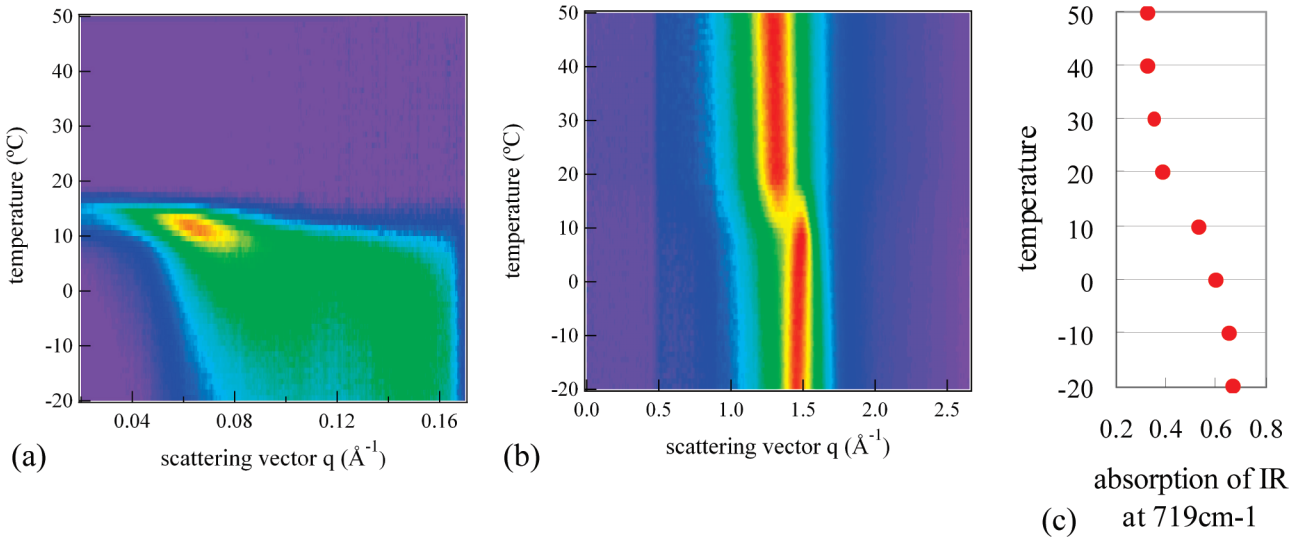

Figure 1. (a, b) Contour plots showing the changes of SAXS (a) and WAXS (b) profiles of EB21 during cooling at a rate of 10 °C/min. (c) Changes in the 719 cm^{-1} IR band at the same cooling rate.

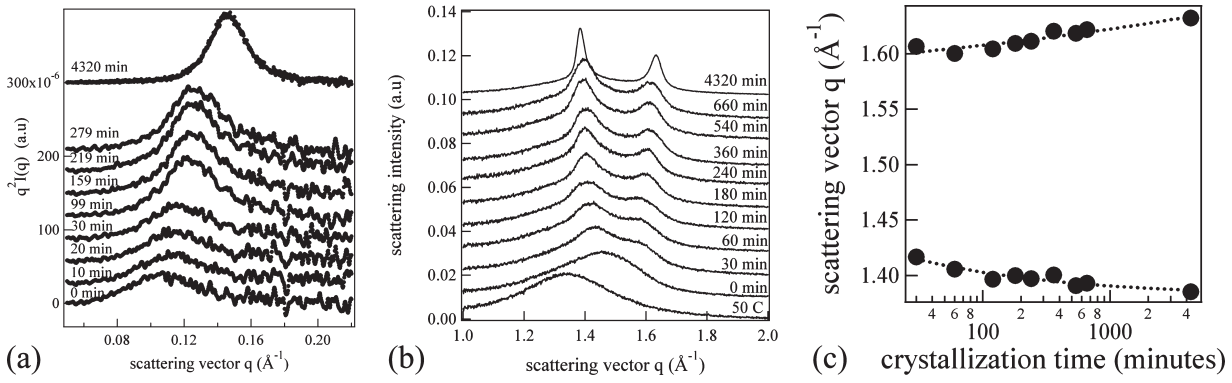

Figure 2. Changes of SAXS (a) and WAXS (b) profiles of HB21 during isothermal crystallization at 1 °C. The shift of peak positions in WAXS is plotted in (c). The exposure time for SAXS and WAXS measurement was 5 min, and data acquired in the first 5 min is described as "0 min" and data taken during 10−15 min of crystallization time is described as "10 min".

Infrared spectra were also obtained at 10 °C intervals as samples having the same thermal history described above were cooled from 50 to −20 °C at 10 °C/min. As shown in Figure 1c, there was a sizable increase in the absorbance of the 719 cm^{-1} band, indicating an increase in the trans conformation in EB21 at the phase transition temperature. The behavior is very similar to that in HB21. Below the phase transition temperature, EB21 and HB21 both have a densely packed and trans-rich structure with birefringence, which is likely to be a hexagonal phase with low packing order.

Next, to clarify the stability of the hexagonal phase, isothermal crystallization experiments were performed for HB21 and EB21 at the phase transition temperature observed in the DSC during the cooling ramp. The polymers were initially held at 50 °C for 10 min, cooled to 1 and 10 °C, respectively, at a rate of 130 °C/min, and then held at each temperature. The structural changes during isothermal crystallization were measured by SAXS and WAXS. As shown in Figure 2a, the development of SAXS in HB21 was very simple; the long period monotonically decreased to 43 Å after 4320 min. The WAXS profiles in Figure 2b show the gradual growth of two Bragg peaks after the rapid shift of the amorphous halo. These results indicate that the hexagonal phase initially formed is a *transiently formed* ordered mesophase. It also is interesting to focus attention on the changes in the positions of the WAXS peaks. As shown in Figure 2c, the two WAXS peaks are gradually shifted in opposite directions. The peak positions were obtained after the subtraction of the amorphous and hexagonal phase contributions from the raw profile data. The stronger peak at about q = 1.42 Å^{-1} shifts to smaller angle, while the weaker peak at about q = 1.60 Å^{-1} shifts to wider angle. In WAXS of crystalline structures, the diffraction intensity usually increases without any shift of peak position during isothermal crystallization.

The peak shift behavior observed in HB21 was also reported for the rotator phase of *n*-alkanes with 20 < *n* < 26 during cooling.[15,16] While the *n*-alkanes are cooled from the melt, the hexagonal rotator phase (R_{II}) initially appears, followed by the transition to the distorted orthorhombic rotator (R_I) phase. Only one scattering peak (100 reflection) is observed in the R_{II} phase, while two peaks (110 and 200 reflections) are observed in the R_I phase, where the respective peaks of 110 and 200 reflections appear at smaller and wider scattering angle than that of 100

dx.doi.org/10.1021/ma200145k |*Macromolecules* 2011, 44, 4030–4034

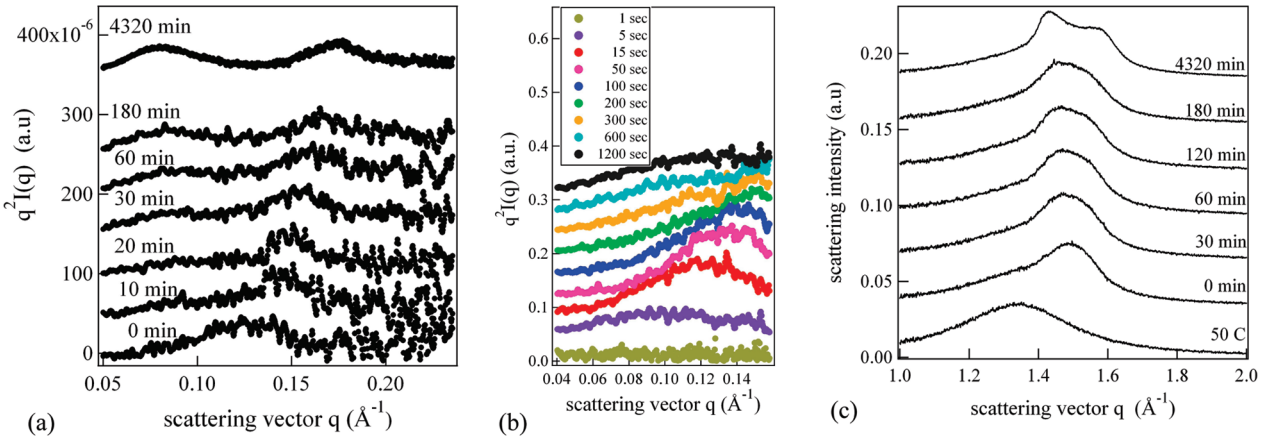

Figure 3. Changes in the SAXS (a), detailed SAXS pattern changes in the first 20 min (b), and WAXS (c) profiles of EB21 during isothermal crystallization at 10 °C. The exposure time for SAXS and WAXS measurement was 5 min, and data acquired in the first 5 min is described as "0 min" and data taken during 10−15 min of crystallization time is described as "10 min".

reflection in the hexagonal phase. The WAXS peak positions of the 110 and 200 reflections in the R_I phase drastically shift in opposite directions during the cooling, and the lattice size difference between the *a*-axis and *b*-axis decreases, as is observed in HB21 isothermal crystallization. Furthermore, it was recently reported that the dynamics of precisely branched PE is similar to that of the rotator phase in *n*-alkanes.[17] Thus, the two WAXS peaks of HB21 seem to be similar to the 110 and 200 reflections of the R_I phase. Initial transient formation of the hexagonal phase, which is similar to the R_{II} phase, is followed by gradual conversion to a distorted orthorhombic phase, which is similar to the R_I phase, to optimize the lattice structure. In mixed *n*-alkanes,[18] the R_{II} (hexagonal and nontilted rotator) phase is stabilized. It appears over a wider temperature range, resulting in the appearance of a broad and single-peak WAXS pattern, which is similar to that of the hexagonal phase in precisely branched PE.

The principal effect of an *n*-alkane mixture is considered to be production of a more disordered interlayer interface. In precisely branched PE, the transient hexagonal phase may have a hexagonal structure with disordered interface like the disordered R_{II} phase in the mixture of *n*-alkanes. Then, through isothermal annealing, the interface of precisely branched PE may become smoothly ordered, and the distorted orthorhombic phase may be gradually more preferred. Furthermore, Strobl showed that the crystallization line of PE coincides with the stability range of the rotator phase in *n*-alkanes.[9] It seems plausible to consider that the transient phase in precisely branched PE is similar in behavior to the rotator phase in *n*-alkanes. However, it is noted that ADMET-PE should be carefully compared with an *n*-alkane and the mixture. The change in peak positions of the 110 and 200 reflections in the rotator phase of *n*-alkanes occurs during cooling/heating and is related to the thermal expansion, where the structure reached at each temperature is an equilibrium state. On the other hand, in HB21, the ordering occurs under isothermal crystallization. From this viewpoint, the structural change in ADMET-PE during mesophase mediated isothermal crystallization seems to correspond to the "gradual densification" during isothermal crystallization, if the analogy between *n*-alkanes and ADMET-PE is correct. The existence of "gradual densification" should be carefully verified with peak assignments based on the crystal structure determination.

In EB21 isothermal crystallization, an interesting nanoscale structural formation was observed in the SAXS profiles, shown in Figure 3a,b. Data in Figure 3a were recorded by using a laboratory X-ray source, while those in Figure 3b were recorded using a synchrotron X-ray source under the same isothermal crystallization conditions in order to obtain the time-resolved data with much shorter intervals in the initial stage. From Figure 3a,b, it is clearly observed that the long period initially decreased, followed by the gradual appearance of a larger long period. In the final stage, the intensity of larger long period was almost comparable to that of the smaller long period; after 4320 min the lengths of the larger and smaller long periods were 78 and 36 Å, respectively. The WAXS data in Figure 3c also indicate that the hexagonal phase is transient, although the crystalline transition from the hexagonal phase to the distorted orthorhombic phase is very slow. In EB21, the SAXS and WAXS changes in the initial stage were measured by using a synchrotron X-ray source (see Figure 4a,b). Here, it is clearly shown that hexagonal phase is grown in the initial stage of isothermal crystallization, followed by the slow packing optimization. The WAXS pattern of EB21 after 4320 min resembles that for HB21 after 30 min.

In EB21, many of the ethyl branches may be initially excluded from the hexagonal phase region due to the *kinetic disadvantage* of including the SCB, resulting in initial formation of a thin-layered hexagonal structure. In the subsequent thickening process, this is replaced by a structure with thicker layers without a further ordering of the packing, which will be related to the layer thickening in PE by the α-process. This occurs by involving more ethyl branches into the layered structure. The lamellar thickness of EB21 after 4320 min crystallization at 10 °C was about 55 Å by TEM,[19] almost twice the length of a 21-carbon chain. Thus, it is expected that all the lamellar stems include, on average, one ethyl branch. After relatively rapid (20−30 min at 10 °C) formation of the larger long periodic structure in EB21, the hexagonal phase changes slowly to the distorted orthorhombic-like phase, which is only barely present after the first 30 min.

On the other hand, in HB21, the exclusion of the hexyl branch was evidenced by the previous TEM observation that the crystal thickness after 4320 min crystallization at 1 °C was about 25−26 Å,[19] which is comparable to the length of a 21-carbon chain with all-trans conformation. The simple decrease in long period also supports the view that the thickening phenomenon observed

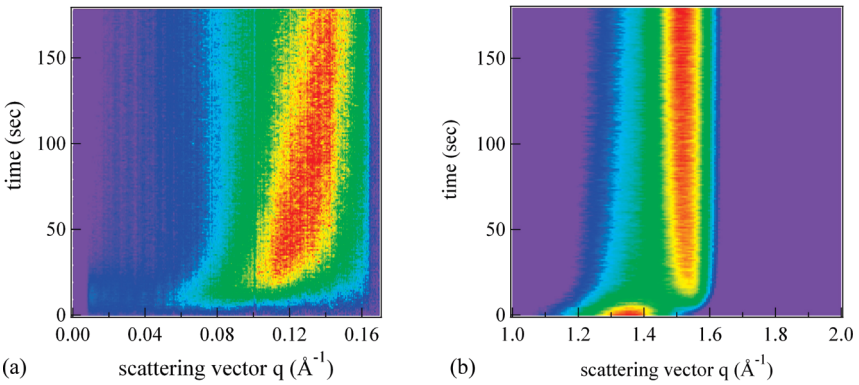

Figure 4. SAXS (a) and WAXS (b) changes in the initial stage of isothermal crystallization of EB21 at 10 °C.

in EB21 does not occur in HB21. This agrees well with the observation of 20 Å at 1 °C on the crystallization line of PE.[20]

Similar differences between PEs with different sized branches have also been noted by other investigators. Hosoda et al.[21] found that for ethyl branches the SCB is partially incorporated into the crystalline region of PE, while branches longer than four carbons are not significantly incorporated into the crystal. Furthermore, from DSC data of precisely branched PE, inclusion of methyl, ethyl, and propyl branches into the crystal and exclusion of branches larger than propyl were indicated.[22]

Our experimental results indicate that ordered mesophase formation is drastically accelerated by introducing the SCB precisely and periodically. Random EB copolymers, even at high butene content (~16 mol %), showed no evidence of a mesophase, and the only observed crystal morphology was an ordered orthorhombic structure.[23] We also investigated the isothermal crystallization behavior of a random ethylene−butene copolymer (EBc) having a similar T_c and polymerized by a single-site metallocene catalyst system. The weight-average molecular weight (M_w) and the distribution (M_w/M_n) were 170 000 and 2.0, respectively, and the number of short chain branched carbons was 79 per 1000 carbon. The observed crystallization peak temperatures (T_c) during cooling at a rate of 10 °C/min by DSC were T_c= 14.5 °C, ΔH_c = 31.5 J/g, while the endothermic curve during heating at a rate of 10 °C/min was very broad, making it difficult to determine the peak melting temperature. The maximum melting temperature was about 60 °C.

Next, we observed isothermal crystallization behavior of EBc. The EBc was initially held at 100 °C for 10 min. It was then cooled to 14.5 °C at a rate of 130 °C/min and then held for isothermal crystallization. The structural changes during isothermal crystallization were measured by WAXS (see Figure 5a). During isothermal crystallization, the WAXS profile changed slightly. To see these changes more clearly, the diffraction from the crystalline structure was extracted by subtracting the amorphous halo from the WAXS profiles (see Figure 5b). The profile of the amorphous phase in EBc is the same as those in EB21 and HB21. After 6 s isothermal crystallization, very disordered structure formation was observed by WAXS. The shape of the extracted diffraction at 6 s is asymmetric and does not appear to be a hexagonal phase. The structure evolution was almost finished in first 10 min, and the WAXS profiles at t = 10 min and t = 60 min were almost same. The extracted diffraction at 10 min crystallization shows two broad peaks, which indicate a loose orthorhombic crystal formation. Thus, it is considered that the disordered (or small-sized) orthorhombic crystal was quickly formed and

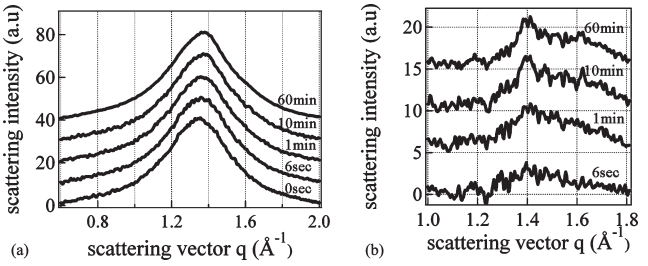

Figure 5. (a) Changes of WAXS profiles during isothermal crystallization (T_c = 14.5 °C) of EBc. (b) Extracted diffraction from the crystalline structure obtained by subtracting the amorphous halo. Profiles are offset for a better view.

the slower ordering (or growing) process of chain packing followed during isothermal crystallization of EBc at 14.5 °C. This rapid formation of a disordered (or small-sized) crystal may be similar to that of the blocklike native crystal suggested by Strobl.[9]

It should be noted that in EBc the crystallization process was relatively rapid and the transient hexagonal phase was not clearly observed. The behavior under high pressure is similar to that at low temperature, and the appearance of a hexagonal phase in ADMET-PE in the very low temperature region may be analogous to the appearance of a hexagonal phase in PE and branched alkanes under high pressure.[24,25] However, from the isothermal crystallization of EBc, it is found that the low temperature environment itself is not sufficient for hexagonal phase formation. The large difference between EBc and EB21 may be explained by the ethylene sequence length distribution. In the case of randomly branched polyethylene, variation in the intrachain chemical composition strongly affects the kinetics of crystallization and the distribution of lamella thickness.[26−29] By AFM observation, it was reported that even in metallocene PE with a narrow interchain chemical composition distribution, crystallization starts from the folding of the longest ethylene sequences, in which the thickest lamellae crystallize, and this is followed by the crystallization of the shorter sequences.[28] In such a case, longer ethylene sequences can fold and crystallize without any disturbance by short chain branches, and a stable nucleus of an orthorhombic crystal is formed. Once nucleation occurs, only the surrounding longer ethylene sequences attach to the growth front, and the shorter ethylene sequences are excluded to the amorphous region between crystalline lamellae; i.e., the fractionation of ethylene chain sequences occurs at the growth front during the crystallization process. The suppression of crystallization in a

random copolymer will be partially caused by the kinetics of the fractionation process. On the other hand, when the branches are precisely placed in chains, there is no ethylene sequence which can crystallize rapidly at higher temperature because all branches are spaced by the same number of carbons. Thus, the crystallization is evenly suppressed in all the ethylene sequences. As a result, mesophase formation by cooperative chain alignment may occur previous to crystallization, in order to release the conformational stress under the strong influence of short chain branches. This mesophase has a long lifetime due to the time-consuming process of optimizing the positions of the short chain branches to form energetically favored stable crystals.

In summary, the formation of a transient ordered mesophase and subsequent crystallization through packing optimization, quite similar to rotator phase formation in *n*-alkanes, was observed when EB21 and HB21 were isothermally crystallized at their crystallization temperatures. The presence of a periodic disturbance in the polymer chains plays an important role in transient ordered mesophase formation even in a flexible polymer, and the kinetic pathway is strongly affected by the size of the branch. Formation of the ordered mesophase is drastically accelerated when the periodic disturbance is introduced into the polymer chain. This methodology provides a new strategy for controlling the formation of an ordered mesophase.

■ ASSOCIATED CONTENT

Supporting Information. Experimental details. This material is available free of charge via the Internet at http://pubs.acs.org.

■ AUTHOR INFORMATION

Corresponding Author

*E-mail: nozue@sc.sumitomo-chem.co.jp (Y.N.); wagener@chem.ufl.edu (K.B.W.).

Present Addresses

[&]Corporate Planning and Coordination Office, Sumitomo Chemical Co. Ltd., Shinkawa 2-27-1, Chuo-ku, Tokyo , Japan.

[§]Department of Chemistry and Materials Science Program, University of New Hampshire, Durham, NH 03834, United States.

[∥]Colombian Sugarcane Research Center, Calle 58 norte No. 3BN-110 Cali, Colombia.

[⊥]DSM Ahead, PO Box 18, 6160 MD, Geleen, Netherlands.

■ ACKNOWLEDGMENT

Y.N. thanks Dr. Y. Shinohara (Univ. of Tokyo) for fruitful discussions about *n*-alkane crystallization. We thank the Photon Factory Advisory Committee (Tsukuba, Japan). We also thank the National Science Foundation for their partial support of this research.

■ REFERENCES

(1) Broadhurst, M. G. *J. Res. Natl. Bur. Stand., Sect. A* **1962**, *66*, 241.
(2) Snyder, R. G.; Maroncelli, M.; Qi, S. P.; Strauss, H. L. *Science* **1981**, *214*, 188.
(3) Doucet, J.; Denicolo, I.; Craievich, A.; Collet, A. *J. Chem. Phys.* **1981**, *75*, 5125.
(4) Sirota, E. B.; Herhold, A. B. *Science* **1999**, *283*, 529.
(5) Imai, M.; Kaji, K.; Kanaya, T. *Macromolecules* **1994**, *27*, 7103.
(6) Matsuba, G.; Kanaya, T.; Saito, M.; Kaji, K.; Nishida, K. *Phys. Rev. E* **2000**, *62*, 1497.
(7) Rastogi, S.; Hikosaka, M.; Kawabata, H.; Keller, A. *Macromolecules* **1991**, *24*, 6384.
(8) Keller, A.; Hikosaka, M.; Rastogi, S.; Toda, A.; Barham, P. J.; Goldbeck-wood, G. *J. Mater. Sci.* **1994**, *29*, 2579.
(9) Strobl, G. *Eur. Phys. J. E* **2005**, *18*, 295.
(10) Smith, J. A.; Brzezinska, K. R.; Valenti, D. J.; Wagener, K. B. *Macromolecules* **2000**, *33*, 3781.
(11) Sworen, J. C.; Wagener, K. B. *Macromolecules* **2007**, *40*, 4414.
(12) Rojas, G.; Wagener, K. B. *Macromolecules* **2009**, *42*, 1934–1947.
(13) Rojas, G.; Berda, E. B.; Wagener, K. B. *Polymer* **2008**, *49*, 2985–2995.
(14) Rastogi, S.; Kurelec, L.; Lemstra, P. J. *Macromolecules* **1998**, *31*, 5022.
(15) Gang, H.; Gang, O.; Shao, H. H.; Wu, X. Z.; Patel, J.; Hsu, C. S.; Deutsch, M.; Ocko, B. M.; Sirota, E. B. *J. Phys. Chem. B* **1998**, *102*, 2754.
(16) Ungar, G. *J. Phys. Chem.* **1983**, *87*, 689.
(17) Wei, Y.; Graf, R.; Sworen, J. C.; Cheng, C. Y.; Bowers, C. R.; Wagener, K. B.; Spiess, H. W. *Angew. Chem., Int. Ed.* **2009**, *48*, 4617.
(18) Sirota, E. B. *Langmuir* **1997**, *13*, 3849.
(19) Hosoda, S.; Nozue, Y.; Kawashima, Y.; Utsumi, S.; Nagamatsu, T.; Wagener, K. B.; Berda, E. B.; Rojas, G.; Baughman, T. W. *Macromol. Symp.* **2009**, *282*, 50.
(20) Cho, T. Y.; Heck, B.; Strobl, G. *Colloid Polym. Sci.* **2004**, *282*, 825.
(21) Hosoda, S.; Nomura, H.; Gotoh, Y.; Kihara, H. *Polymer* **1999**, *31*, 1990.
(22) Rojas, G.; Inci, B.; Wei, Y.; Wagener, K. B. *J. Am. Chem. Soc.* **2009**, *131*, 17376.
(23) Hu, W.; Srinivas, S.; Sirota, E. B. *Macromolecules* **2002**, *35*, 5013.
(24) Rastogi, A.; Hobbs, J. K.; Rastogi, S. *Macromolecules* **2002**, *35*, 5861.
(25) Rastogi, A.; Terry, A. E.; Mathot, V. B. F.; Rastogi, S. *Macromolecules* **2005**, *38*, 4744.
(26) Hosoda, S. *Polym. J.* **1988**, *20*, 383.
(27) Crist, B.; Mirabella, F. *J. Polym. Sci., Polym. Phys.* **1999**, *37*, 3131.
(28) Mirabella., F. J. *J. Appl. Polym. Sci.* **2008**, *108*, 987.
(29) Hosoda, S.; Nozue, Y.; Kawashima, Y.; Suita, K.; Seno, S.; Nagamatsu, T.; Wagener, K. B.; Inci, B.; Zuluaga, F.; Rojas, G.; Leonard, J. K. *Macromolecules* **2011**, *44*, 313.